Journal of Solid State Chemistry **154,** 13–19 (2000)
doi:10.1006/jssc.2000.8804, available online at http://www.idealibrary.com on IDEAL®

Thermoelectric Properties of Metal-Doped β-Rhombohedral Boron

Takahiro Nakayama,*[,1,2] Junichiro Shimizu,†[,3] and Kaoru Kimura*[,†]

*Department of Advanced Materials Science and †Department of Materials Science, University of Tokyo, 7-3-1 Hongo, Bunkyo-ku, Tokyo 113-8656, Japan

Received September 9, 1999; in revised form April 25, 2000; accepted May 1, 2000

β-Rhombohedral boron (β-rh. boron) was doped with V, Cr, Fe, Co, or Zr to investigate the relationship between occupancies of the doping sites and thermoelectric properties. Doping with V or Cr, which preferentially occupy the A_1 sites, produces an increase in electrical conductivity and a negative Seebeck coefficient, while doping with Fe or Co, which occupy the A_1 and D sites equally, also increases the electrical conductivity though the Seebeck coefficient remains positive. Doping with Zr, which does not occupy the A_1 sites, slightly increases the electrical conductivity with a resultant larger Seebeck coefficient. Regarding Co- and Zr-doubly doped *p*-type β-rh. boron, both properties are determined mainly by Co content. The observed temperature dependence of the electrical conductivity of metal-doped β-boron clearly indicates variable range hopping conduction such that both properties increase with increasing temperature up to room temperature, in contrast to the behavior of ordinary metals and semiconductors. The power factors of Co-doped *p*-type β-rh. boron and V- or Cr-doped *n*-type β-rh. boron increased with increasing temperature, and doping with about 1 at.% metal atoms produced materials whose power factor at room temperature is three to four orders of magnitude larger than that of pure β-rh. boron. Finally, 1 at.% Co doping decreased the thermal conductivity of β-rh. boron from 16 to about 4–2 W/m · K, with the maximum ZT of *p*-type $Co_{1.0}B_{105}$ being subsequently estimated as 1.0×10^{-6} at room temperature. © 2000 Academic Press

Key Words: **β-rhombohedral boron; metal doping; electrical conductivity; Seebeck coefficient; site occupancy; hopping conduction; power factor; figure-of-merit; covalent–metallic bonding conversion; electron–phonon interaction.**

I. INTRODUCTION

The pioneering research carried out in the late 1950s on semiconductor thermoelements and thermoelectric (TE) cooling by Ioffe (1) proved to be a technology springboard in this field. With respect to semiconductor TE energy conversion, his main principle has been particularly useful in systematically studying semiconductors with large carrier mobility or large effective mass. As this principle is derived from the Boltzmann transport equation using the relaxation time approximation (1–3), only the carrier concentration is used to uniquely determine the electrical conductivity σ, Seebeck coefficient S, and electron part κ_{el} of thermal conductivity κ. TE materials investigated and optimized using this principle have thus far demonstrated insufficient performance, and also, the principle cannot explain the transport properties of a number of materials with a large electron correlation or large electron–phonon interaction. On the other hand, some materials with small carrier mobility such as oxides (4) and borides (5–9) are known to exhibit high performance above room temperature, which implies the existence of new leading principles concerned with carrier localization.

Boron-rich solids are semiconductors because they consist mainly of B_{12} icosahedral clusters, which have three-centered covalent bonds owing to their electron deficiency, and because the electronic structure near the bandgap is closely related to these clusters (10). Boron-rich semiconductors have an extremely high melting point (> 2300 K) due to the strong bonds of intra- and interclusters (11), a characteristic that allows them to function at high temperatures. Their thermal conductivity is quite low because the network of B_{12} clusters, i.e., the fivefold symmetry of B_{12} icosahedral clusters, is complex and markedly different compared with the rotational symmetry of crystals. β-Rhombohedral boron (β-rh. boron). (6), boron carbides (5), α-AlB_{12} (6), and boron silicides (8, 9) all have large S values and exhibit relatively high performance as a *p*-type TE material at > 800 K. The TE properties of β-rh. boron can also be altered by doping metals into interstitial sites.

The values of σ and S for semiconducting β-$FeSi_2$ phase simultaneously increase by mixing with metallic ε-$FeSi_2$ phase (12). Therefore, if metallic bonding and covalent bonding can locally coexist, i.e., if materials are developed having an electrical conductivity as high as that of metals and a Seebeck coefficient as high as that of semiconductors, then semiconductor TE energy conversion can be enhanced. As the bonding nature of B_{12} clusters is convertible from

[1] JSPS Research Fellow.

[2] To whom correspondence should be sent at the present address: Angstrom Technology Partnership, Joint Research Center for Atom Technology.

[3] Present address: Hitachi Co. Ltd.

0022-4596/00 $35.00

covalent to metallic bonds by changing the environment of intra- or interclusters (13), an electronic state optimized by the design of the bonding nature of individual clusters, as well as that of the arrangement of clusters, could realize a substantial improvement in the TE properties of boron-rich solids.

Such a possibility led to the present study in which we investigate how to control the electrical properties of β-rh. boron by doping β-rh. boron with several kinds of metals. In addition, we propose new principles for similar materials with localized carriers.

II. EXPERIMENTAL

β-Rh. boron was doped with V, Cr, Fe, Co, or Zr (99.9% pure), each of which is known to occupy only two kinds of sites (14–17) of the three kinds of interstitial doping sites ($A_1/D/E$) in a β-rh. boron structure (18). Briefly, a mixture of amorphous boron (99.9% pure) and each metal, except V, was subjected to arc-melting in which samples were homogenized by placing them in a h-BN crucible and annealing under an Ar atmosphere at 2073 K for 48 h. The V-doped sample was annealed at 1473 K for 96 h. Excess metals were etched by hydrochloric acid. Direct-current conductivity and Seebeck coefficient measurements were performed using sliced polycrystalline bulk samples, with X-ray powder diffraction (XRD) measurements being performed on the remaining sample after crushing.

Crushed powder samples were mounted on a substrate made of a SiO_2 single crystal (Rigaku Co., Ltd.) which did not allow reflection of Cu$K\alpha$ rays in the 2θ range of 5–150°. XRD data were collected at room temperature using Cu$K\alpha$ rays in the 2θ range of 10°–80°. Samples were successively mixed with Si to provide an internal calibration standard, and XRD data for determining the lattice constants were collected in the 2θ range of 37°–57° as there are few overlapping peaks in this region. Both data sets were analyzed in turn by the Rietveld method using the RIETAN-97β code (19); i.e., the sets were fit using the same structural parameters such that the lattice parameters and occupancies of the doping sites could be determined. The coordination and isotropic thermal vibrational parameter of each site were slightly changed by being fit to single-crystalline structural analysis data reported previously (14–17).

We investigated the respective relationship between the Rietveld analysis-determined occupancy of each doping site and the electrical properties, electrical conductivity, and Seebeck coefficient. The dc electrical conductivity was measured from 20 to 300 K using the van der Pauw method, while the Seebeck coefficient was measured using a stable temperature difference from 200 to 300 K.

The thermal diffusivity of 1-mm-thick sample slices was measured using the laser flash method, after which the thermal conductivity was estimated under the assumption that the sample's specific heat is equal to that of pure β-rh. boron (20).

III. RESULTS AND DISCUSSION

1. Occupancies of Doping Sites

The unit cell of β-rh. boron consists of a B_{12} framework, a vertex B_{12} cluster and three edge-center B_{12} clusters, and a B_{28}–B–B_{28} chain with nearly 105 boron atoms (21), which is why it is often referred to as B_{105}. Another model assumes it consists of a B_{84} framework and B_{10}–B–B_{10} chain, where the B_{84} "soccerball" cluster has a multishell structure in which the vertex B_{12} cluster forms the first shell, another B_{12} cluster forms the second shell, and a B_{60} soccerball cluster forms the third shell. The 20 A sites in a B_{84} cluster, i.e., 2 A_1, 6 A_2, and 12 A_3 sites, are truncated tetrahedral sites situated dodecahedrally around the B_{12} second shell such that they form a triacontahedral cluster with the second shell, and the A_1 site is surrounded by a vertex B_{12} cluster and three edge-center B_{12} clusters. Doping into the A_1, D, and E sites, respectively, corresponds to doping into the B_{84} soccerball cluster, interstices of the B_{10}–B–B_{10} chain, and interstices of four B_{84} clusters.

Rietveld analysis confirmed that (i) metal atoms are interstitially doped into β-rh. boron, i.e., the cell volume of each metal-doped β-rh. boron sample M_xB_{105} (M = V, Cr, Fe, Co, or Zr) is larger than that of pure β-rh. boron, and (ii) a single phase is present in the range $x \leq 1.0$. Figure 1 is a scanning electron microscope (SEM) image of $Cr_{2.5}B_{105}$, where a small amount of the second phase, being a eutectic phase of two different Cr–B compounds, is dispersed throughout the Cr-doped β-rh. boron matrix. From the occupational analysis shown in Figs. 2 and 3, it was found that V/Cr atoms occupy the A_1 site two to three times more preferentially than the D site, whereas the number of Fe/Co atoms in the A_1 site is nearly the same as that in the D site; and in Zr-doped β-rh. boron, Zr atoms occupy the D and E sites. Taken together these results indicate that V and Cr and not Zr preferentially occupy the site in the B_{84} soccerball clusters, and that Co and Fe occupy both the site in the B_{84} clusters and that around –B_{10}–B–B_{10}– chains. It should be noted that these occupational trends are consistent with those obtained using single-crystalline structural analysis on VB_{65} (14), CrB_{41} (15), FeB_{49} (16), and ZrB_{51} (17).

Using the maximum entropy method in combination with the Rietveld method, we previously reported the electron density distribution in α-rh. boron (11). The same approach is now in progress to analyze pure and metal-doped β-rh. boron compounds such that observation of local metallic–covalent bonding conversion of B_{12} clusters is realized.

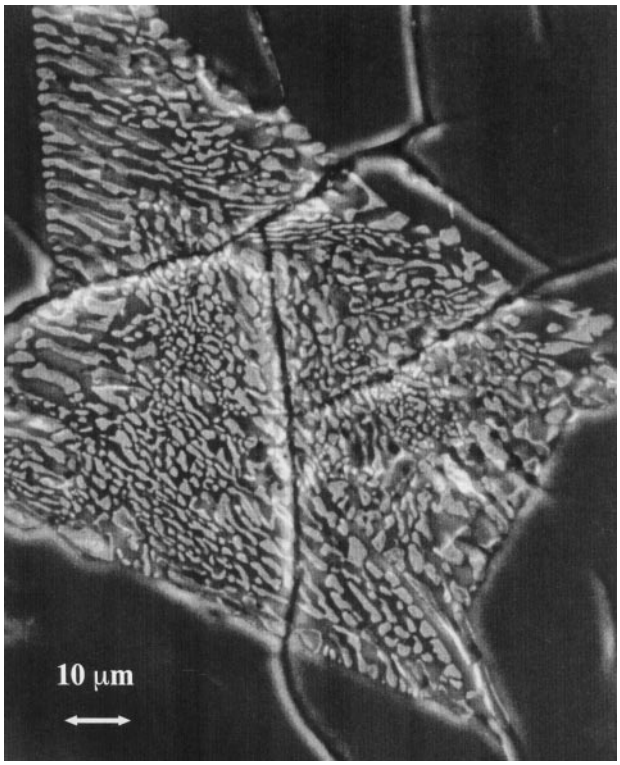

FIG. 1. Scanning electron microscope (SEM) image of $Cr_{2.5}B_{105}$.

2. *Composition Dependence of Electrical Conductivity and Seebeck Coefficient*

According to Ioffe's leading principle, the efficiency of the TE energy conversion is determined by the dimensionless figure-of-merit ZT in which Z is a material parameter called figure-of-merit expressed as

$$Z = S^2\sigma/\kappa, \qquad [1]$$

and T is the temperature at which the material is used. Materials with a large S, a large σ, and a small κ are thus candidates for TE materials.

Doping with V, Cr, Fe, Co, Ni, or Cu results in the A_1 sites being occupied by doped atoms such that the electrical conductivity of β-rh. boron is increased, being a remarkable effect for V and Cr which preferentially occupy the site. Figure 2 shows how varying x in Cr_xB_{105} affects σ, S, and site occupancy. Due to the sharp increase in both σ and the occupancy of the A_1 site for $x \leq 1.0$, the rise in σ is attributed to dopants occupying the A_1 site. In the two-phase region $x \geq 1.5$, however, σ no longer increases due to the reduction in the Cr concentration. This occurs because the appearance of the second phase reduces the Cr concentration in β-rh. boron matrix. As doping with Zr does not result in occupation of the A_1 site, only a slight increase in σ occurs (Fig. 4).

The effect of composition on S is also closely related to A_1 site occupancy, since S decreases with increasing occupancy, and since a transition from p- to n-type occurs by doping with about 1 at.% Cr or V. Doping with Co, which occupies equally the A_1 and D sites, decreases S and it remains positive (Fig. 4b) even in the two-phase region $x \geq 1.5$, while doping with Zr, which can occupy only the D and E sites, increases S with increasing Zr concentration. As the carrier concentration dependence of S generally shows a tendency opposite that of σ in ordinary metals and semiconductors obeying Ioffe's leading principles, increases in both σ and S of Zr-doped β-rh. boron are thought to be attributed to a kind of hopping conduction described later.

Based on X-ray photoemission spectroscopy (XPS) and electron energy loss spectroscopy (EELS) measurements of pure and Li- and V-doped β-rh. boron (13, 22), we reported that V atoms, hybridizing B atoms at the bottom of the conduction band so that the band gap is reduced, increase the density of states at the Fermi level, $N(E_F)$, whereas such effects do not occur in Li-doped β-rh. boron since Li does not occupy the A_1 site. Since an A_1 site is surrounded by 12 B atoms, with the distances from the A_1 site being almost equal, this structure resembles that of the center of a B_{12} icosahedral cluster. If an atom is then inserted into the center of a B_{12} icosahedral cluster so that a B_{13} cluster is formed, then a covalent–metallic bonding conversion can occur (13, 23, 24). The hybridization caused by occupying the A_1 site with V implies a local bonding conversion from covalent to metallic around the site. Accordingly, the

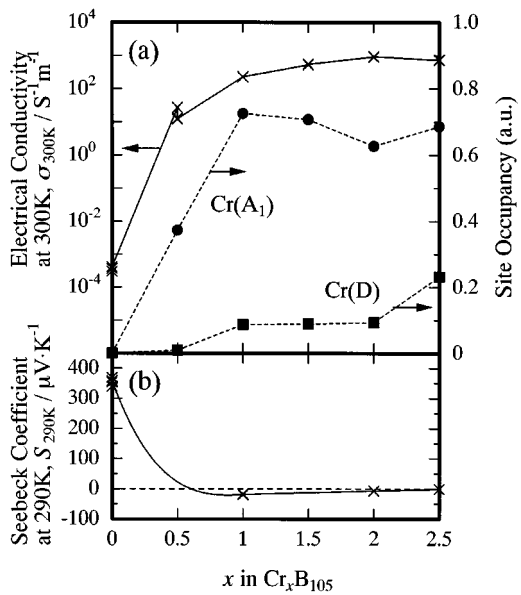

FIG. 2. Cr concentration dependence of electrical properties and site occupancies for Cr-doped β-rhombohedral boron. (a) Electrical conductivity at 300 K together with the occupancies of the doping sites. (b) Seebeck coefficient at 290 K.

increase in σ by doping with V or Cr can be explained as follows: hybridization of a dopant atom occupying the A_1 site with boron atoms around it occurs, i.e., covalent–metallic local conversion, so that the locally metallic region increases with an increase in the dopant concentration. Moreover, the transition from p- to n-type implies that the dopants occupying the A_1 site produce n-type carriers.

Li exhibits the same occupational trend (25) as Zr in that the electrical conductivity of Li- and Zr-doped β-rh. boron slightly increases with an increase in the dopant concentration (26–28), and $N(E_F)$ shows no substantial increase. It is therefore considered that near the band edge Zr atoms do not hybridize with B atoms around them. This is different from the case in which an increase in σ due to increasing the carrier concentration causes S to increase with increasing Zr concentration. Although the exact reason why S increases when doped with Zr is not fully understood, it is hypothesized to be the result of a kind of hopping conduction mechanism. Another possibility is that an expansion of the lattice, or a distortion of clusters by interstitial doping into the site among clusters, causes a change in the dispersion of the density of states. To clarify this, investigations on the band structure using EELS measurements are in progress.

Because σ of β-rh. boron was found to be dependent on the occupancy of the A_1 site, additional experiments were performed. Cr exhibits a slightly different occupational trend compared with Fe, and therefore a series of Cr- and Fe-doubly doped β-rh. boron samples, $Cr_xFe_{1-x}B_{105}$ ($0 \leq x \leq 1$), were prepared to change the atomic ratio of the A_1 to D sites. Figure 3 shows the relationship between the electrical properties and occupancies of the doping sites, where electrical conductivity remains nearly unchanged in the region $x \leq 0.5$. In the range $0.5 < x \leq 1.0$, note that when the number of atoms occupying the A_1 site is larger than that occupying the D site, σ increases and S becomes negative. Since S is positive for $x \leq 0.5$, the dominant carriers are holes. Although σ should decrease with an increase in the Cr concentration because electrons available from Cr atoms occupying the A_1 sites can compensate for the holes, such a compensation is not observed in Fig. 3. It is therefore postulated that dopants occupying the D sites may produce p-type carriers such that tightly localized p- and n-type carriers both contribute to the conduction because Cr and Fe occupying the A_1 site, i.e., hybridizing with B atoms and producing localized states, reduce the bandgap.

Doping with Zr increases S without reducing σ, which implies that σ and S of β-rh. boron are independently controlled, whereas those of ordinary metals and semiconductors are not. Co and Zr are p-type dopants that are different from each other with respect to occupational sites and contribution to electronic properties. As mentioned, Co occupying the A_1 and D sites increases σ, whereas Zr occupying the D and E sites increases S. As a means of individual control of the electrical properties, we prepared

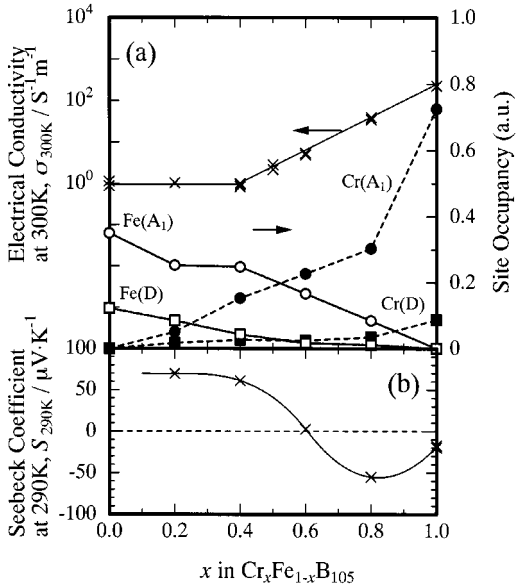

FIG. 3. Cr concentration dependence of electrical properties and site occupancies for Cr- and Fe-doubly doped β-rhombohedral boron. (a) Electrical conductivity at 300 K together with the occupancies of the doping sites. (b) Seebeck coefficient at 290 K.

a series of Co- and Zr-doubly doped β-rh. boron, $Co_xZr_{1-x}B_{105}$ ($0 \leq x \leq 1$). Figure 4 shows their electrical properties, where σ and S are both nearly determined by Co concentration, with Zr addition yielding a slight increase in these properties compared with those of Co_xB_{105}. Co atoms

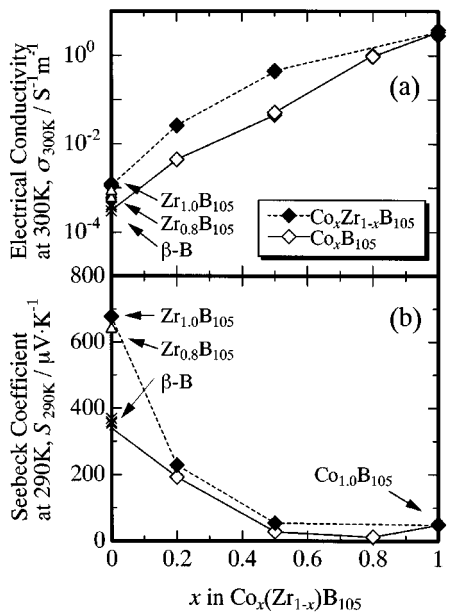

FIG. 4. Co concentration dependence of σ and S for Co- and Zr-doubly doped β-rhombohedral boron: (a) σ at 300 K, (b) S at 290 K.

occupying the A_1 sites and hybridizing with B atoms are considered to produce local metallic bonds around them which strongly affect $N(E_F)$. Individual control of σ and S is therefore precluded, though it should be noted that the tendency for simultaneous increases in σ and S can be produced by Zr addition of not only $x = 0$ but also $x = 0.2$ and 0.5.

3. *Temperature Dependence of Electrical Conductivity and Seebeck Coefficient*

Figure 5 shows the temperature dependence of σ in metal-doped β-rh. boron, which can be explained as variable-range hopping conduction expressed by Mott (29), i.e.,

$$\sigma = \sigma_0 \exp\left\{-\left(\frac{T_0}{T}\right)^{1/4}\right\}, \qquad [2]$$

rather than by (i) phonon-assisted hopping conduction for boron carbides as expressed by Emin and Holstein (30), i.e.,

$$\sigma = \frac{C}{T}\exp\left(-\frac{E}{k_B T}\right), \qquad [3]$$

or (ii) Arrhenius-type conduction for ordinary semiconductors. In these expressions, σ_0 and C are constants, T_0 a constant inverse proportional to $N(E_F)$, and E the thermal activation energy of the mobility of carriers. In Arrhenius-type conduction, due to thermal activation of the concentration of carriers, the electrical conductivity of ordinary semiconductors increases with increasing temperature. On the other hand, σ for hopping conduction expressed by Eqs. [2] and [3] increases with increasing temperature because the mobility of carriers is thermally activated whereas the concentration of carriers is almost constant. Since Mott's law expressed by Eq. [2] can be adapted to disordered systems such as those appearing in amorphous semiconductors, metal-doped β-rh. boron is considered to consist of B_{12} icosahedral clusters with a fivefold symmetry resembling amorphous semiconductors in both structure and electrical properties. Here, the deviation from linearity, especially in the case of V-doped β-rh. boron at temperatures < 200 K, is due to inclusion of a second phase, i.e., a VB_2 metallic phase, the amount of which is insufficient to be detected by XRD. It is already known that without the exception of low temperatures this law reasonably explains the temperature dependence of σ of V-doped β-rh. boron if a VB_2 phase which is contained in a V-doped β-rh. boron sample is etched by a mixture of hydrochloric acid and nitric acid (27). As σ determined by this metallic phase is nearly unchanged with respect to temperature, it is negligiblly small at temperatures as high as room temperature as compared with σ for a V-doped β-rh. boron matrix. Note that σ_0 and $N(E_F)$ can be estimated from T_0 obtained by fitting these lines at parts of high temperatures using Eq. [2], where it is subsequently found that $N(E_F)$ for V, Cr, Fe, and Co dopants occupying the A_1 site will increase with increasing metal concentration, while σ_0 will remain unchanged. Such behavior is consistent with the results of XPS measurements (13) for V-doped β-rh. boron as described above. It is also found that $N(E_F)$ for Zr-doped β-rh. boron remains nearly unchanged.

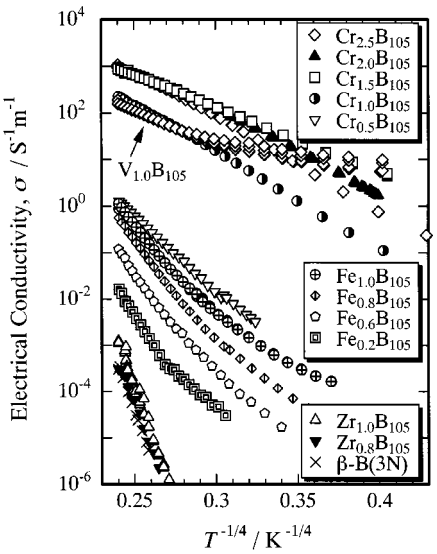

FIG. 5. Temperature dependence of σ for metal-doped β-rhombohedral boron.

The temperature dependence of S for disordered systems in which there occurs phonon-assisted hopping of small polarons has been expressed by Wood and Emin (5) using

$$S = (T\Delta S' + E_T)/qT = A + BT, \qquad [4]$$

where A and B are constants, $\Delta S'$ the change in entropy due to insertion of a carrier, E_T the average vibrational energy, and q the charge of carriers. Brenig *et al.* (31) expressed variable-range hopping conduction using

$$S \approx \frac{k_B^2}{64q} T_0^{1/2} T^{1/2} \{N'(E)/N(E)\}_{E_F} \{1 + (T_0/T)^{1/4}\}, \qquad [5]$$

where $N'(E)$ denotes $\partial N(E)/\partial E$. When the effect of correlation between hopping length and hopping energies is taken into account, Overhof (32) proposed that S is proportional to $T^{1/2}$.

Figure 6 shows the temperature dependence of S for metal-doped β-rh. boron, where, similar to phonon-assisted hopping conduction, S tends to increase linearly with increasing temperature. While this tendency cannot be clearly

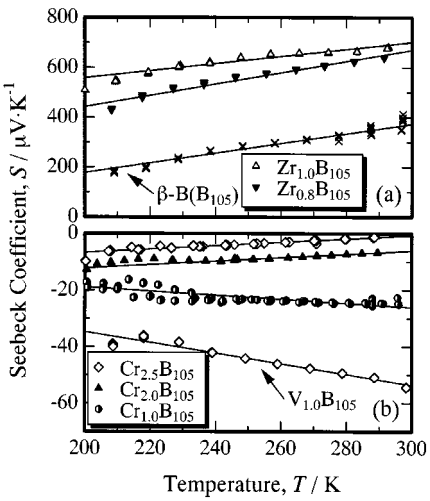

FIG. 6. Temperature dependence of S for metal-doped β-rhombohedral boron.

distinguished from variable-range hopping conduction because the measured temperature range is too narrow, it is definitely different from ordinary semiconductors of the Arrhenius type, and is considered to be attributed to a kind of hopping conduction caused by an electron–phonon interaction. Measurements covering a wider temperature range should be able to clarify how S is expressed for metal-doped β-rh. boron. Moreover, further investigations are in progress to determine whether the carriers that determine S are the same as those that determine σ.

Figure 7 shows the temperature dependence of σ for $Cr_xFe_{1-x}B_{105}$ and $Co_xZr_{1-x}B_{105}$ and S for $Cr_xFe_{1-x}B_{105}$, where variable-range hopping-type conduction is again indicated. Note that S for $Cr_{0.6}Fe_{0.4}B_{105}$ changes from positive to negative as temperatures are lowered, behavior that suggests that electrons and holes are both carriers contributing to S due to a reduced bandgap. By taking into account the results from investigations of composition dependence, since no compensation effects were observed, the transport properties of metal-doped β-rh. boron can be reasonably explained using a two-band model in which both electrons and holes move by hopping.

4. *Composition and Temperature Dependence of Power Factor*

The power factor, P, is defined by

$$P = S^2\sigma. \qquad [6]$$

In ordinary metals and semiconductors, σ and S show an opposite tendency with respect to temperature dependence. Figure 8 shows the temperature dependence of P for M_xB_{105}, where P continues to increase up to room temperature, which is not surprising since σ and S both increase with increasing temperature, representative of an electron–phonon interaction. Because the increase in σ by doping with metals overcomes the decrease in S, P for p- or n-type metal-doped β-rh. boron at room temperature is three to four orders of magnitude larger than that of pure β-rh. boron with a dopant concentration of $0.8 \leq x \leq 1.5$ in the case of M_xB_{105}. It should also be noted that P of Zr-doped β-rh. boron increases with increasing Zr concentration due to an increase in both σ and S, i.e., Zr doping or Zr addition produces a situation quite different from ordinary metals and semiconductors whose P values are maximum at a certain carrier concentration.

5. *Thermal Conductivity and Figure-of-Merit*

Doping with metals into β-rh. boron not only increases σ but also reduces κ by affecting impurity scattering of phonons. For example, doping with 1 at.% Co causes the

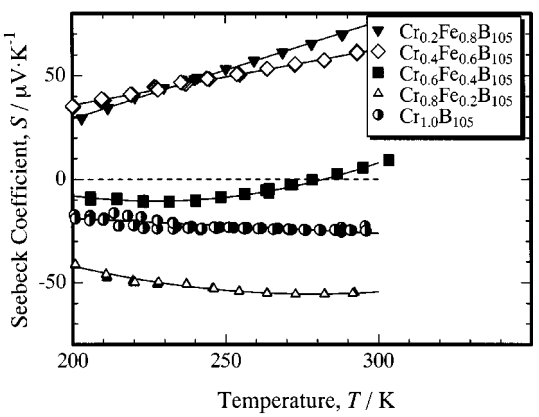

FIG. 7. Temperature dependence of S for Cr- and Fe-doubly doped β-rhombohedral boron.

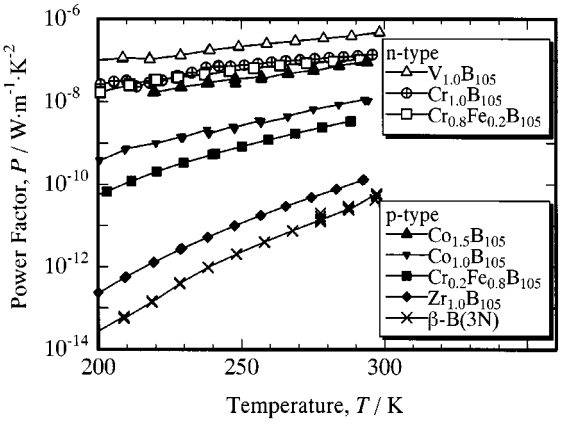

FIG. 8. Temperature dependence of the power factor of metal-doped β-rhombohedral boron.

thermal conductivity of β-rh. boron at room temperature to decrease from 16 to 4–2 W/m·K, values that are also obtained by decreasing the grain size to < 100 mm. The maximum ZT value for p-type $Co_{1.0}B_{105}$ at room temperature is accordingly estimated to be 1.0×10^{-6}. Providing this transport mechanism continues, a further increase in thermoelectric properties can be expected at higher temperatures along with other effects on covalent–metallic bonding conversion.

IV. CONCLUSIONS

The arc-melting method was used to dope V, Cr, Fe, Co, or Zr into β-rh. boron. Based on the relationship between the occupancies of doping sites and electrical conductivity, an increase in electrical conductivity occurs due to dopants occupying the A_1 site; i.e., the Seebeck coefficient decreases with increasing site occupancy. In addition, doping with about 1 at.% V or Cr, which preferentially occupy the site, produces a transition from p- to n-type. Doping with Fe or Co, which occupy the A_1 and D sites equally, also decreases the Seebeck coefficient although it remains positive. In Zr-doped β-rh. boron, the electrical conductivity and Seebeck coefficient both increased with increasing Zr concentration, a behavior that contrasts with that of ordinary metals or semiconductors. A type of hopping conduction is considered to be the responsible mechanism. Since both properties in metal-doped β-rh. boron increase with increasing temperatures, being representative of an electron–phonon interaction, the power factor continues to increase up to room temperature. Most noteworthy, at room temperature (i) the power factor of V-doped n-type and Co-doped p-type β-rh. boron was found to be three to four orders of magnitude larger than that of pure β-rh. boron, and (ii) doping with 1 at.% Co caused the thermal conductivity of β-rh. boron to decrease from 16 to around 4–2 W/m·K. The maximum ZT value for p-type $Co_{1.0}B_{105}$ at room temperature is accordingly estimated to be 1.0×10^{-6}.

ACKNOWLEDGMENTS

Sincere gratitude is extended to M. Nakamura and ULVAC Company Ltd. for valuable assistance in performing SEM and thermal diffusivity measurements. This research was supported by a grant from Iketani Science and Technology Foundation and a Grant-in-Aid for Scientific Research from Japan's Ministry of Education, Science, Sports and Culture.

REFERENCES

1. A. F. Ioffe, "Semiconductor Thermoelements and Thermoelectric Cooling," Infosearch, London, 1956.
2. D. M. Rowe and C. M. Bhandari, "Modern Thermoelectrics," p. 15, Reston, Reston VA, 1983.
3. H. J. Goldsmid, "Electronic Refrigeration," p. 12, Pion, London, 1986.
4. For example, I. Terasaki, Y. Sasago, and K. Uchinokura, *Phys. Rev. B* **56,** R12685 (1997).
5. C. Wood and D. Emin, *Phys. Rev. B* **29,** 4582 (1984).
6. O. A. Golikova, V. K. Zaitsev, V. M. Orlov, A. V. Petrov, L. S. Stilbans, and E. N. Tkalenko, *Phys. Stat. Sol.*, (a) **21,** 405 (1974).
7. G. A. Slack, J. H. Rosolowski, C. Hejna, M. Garbauskas, and J. S. Kasper, *in* "Proceedings 9th International Symposium on Boron, Borides, and Related Compounds, Duisburg, September 21–25, 1987," p. 132.
8. B. Pistourlet, J. L. Robert, J. M. Dusseau, J. M. Darolles, B. Armas, and C. Combescure, *Proc. Int. Solar Electric Conf.* 887 (1967).
9. J. M. Darolles, T. Lepetre, and J. M. Dusseau, *Phys. Status. Solidi A* **58,** K71 (1980).
10. R. Franz and H. Werheit, *AIP Conf. Proc.* **231,** 29 (1991).
11. M. Fujimori, T. Nakata, T. Nakayama, E. Nishibori, K. Kimura, M. Takata, and M. Sakata, *Phys. Rev. Lett.* **82,** 4452 (1999).
12. H. Nagai, S. Katsuyama, S. Nakayama, H. Kobayashi, K. Majima, and M. Ito, *Mater. Trans. JIM* **39,** 515 (1998).
13. K. Kimura, H. Matsuda, M. Fujimori, M. Terauchi, M. Tanaka, H. Kumigashira, N. Yokoya, and T. Takahashi, *in* "Quasicrystals" (S. Takeuchi and T. Fujiwara, Eds.), p. 595, World Scientific, Singapore, 1998.
14. M. F. Gaubauskas, J. S. Kasper, and G. A. Slack, *J. Solid State Chem.* **63,** 424 (1986).
15. S. Andersson and T. Lundström, *J. Solid State Chem.* **2,** 603 (1970).
16. B. Callmer and T. Lundström, *J. Solid State Chem.* **17,** 165 (1976).
17. B. Callmer, L.-E. Tergenius, and J. O. Thomas, *J. Solid State Chem.* **26,** 275 (1978).
18. T. Lundström, *AIP Conf. Proc.* **140,** 19 (1985).
19. F. Izumi, *in* "The Rietveld Method" (R. A. Young, Ed.), Oxford Univ. Press, New York, 1993.
20. P. R. H. Tçrkes, E. T. Swartz, and R. O. Pohl, *AIP Conf. Proc.* **140,** 346 (1985).
21. D. Geist, R. Kloss, and H. Follner, *Acta Crystallogr. Sect. B* **26,** 1800 (1970).
22. M. Terauchi, Y. Kawamata, M. Tanaka, H. Matsuda, and K. Kimura, *J. Solid State Chem.* **133,** 152 (1997).
23. M. Fujimori and K. Kimura, *J. Solid State Chem.* **133,** 310 (1997).
24. M. Fujimori and K. Kimura, *Mater. Japan* **37,** 606 (1998).
25. M. Kobayashi, H. Matsuda, and K. Kimura, *J. Alloys Comp.* **221,** 120 (1995).
26. H. Matsuda, T. Nakayama, K. Kimura, Y. Murakami, H. Suematsu, M. Kobayashi, and I. Higashi, *Phys. Rev. B* **52,** 6102 (1995).
27. H. Matsuda, N. Tanaka, T. Nakayama, K. Kimura, Y. Murakami, H. Suematsu, M. Kobayashi, and I. Higashi, *J. Phys. Chem. Solids* **57,** 1167 (1996).
28. H. Matsuda and K. Kimura, *Hyomen Kagaku* **18,** 156 (1997). [In Japanese.]
29. N. F. Mott, *Philos. Mag.* **19,** 835 (1965).
30. D. Emin and T. Holstein, *Ann. Phys.* **53,** 439 (1969).
31. W. Brenig, G. H. Döhler, and P. Wölfle, *Z. Phys.* **258,** 381 (1973).
32. H. Overhof, *Phys. Status Solidi B* **67,** 709 (1975).